Hydrostatic Transmission with a Traction Control

Massimo Martelli, Luca G. Zarotti

Abstract - **The paper addresses a typical application of the hydrostatic transmissions, i.e. the locomotion of vehicles. It is proved that if a full traction scheme is adopted (with hydraulic motors on both axles) the contribution of the front and rear axle to the overall traction capacity can be changed by acting on the displacement setting of the individual motors. By piloting these degrees of freedom through an automatic control system, the perturbations in the traction balance due to soil properties or vehicle attitude can be compensated.**

Index Terms - **fluid power, hydrostatic transmission, modelling and simulation, traction control.**

I. Introduction

The hydrostatic transmissions have a distinct position in the hydraulic fluid power technology. The primary reason is found in their functional target - i.e. to provide from an input power shaft one or more output shafts running at controlled speed or implementing a given law between torque and speed, within a specified operating envelope - which requires that the transmission be separate from any other hydraulic circuits, just sharing the power of the prime mover.

The simple statement of its function opens the hydrostatic transmissions to several potential applications, but among them the locomotion of vehicles is probably the most interesting one. In fact, the transmission interacts with the engine on one end and with the locomotion devices on the other end (normally wheels, but also tracks sometimes) while receiving direct or indirect commands issued by the vehicle operator. These complex interactions give rise to several problems, e.g. the sizing of the transmission or the management of its dynamic braking, which receive little attention outside the relationships between manufacturers and clients or deserve qualitative remarks in the public literature.

A similar approach seems to the extended to the so called “traction control” problem which can be stated in general terms as *the set of actions taken on the degrees of freedom of the hydrostatic transmission mounted on a wheeled vehicle to modify (automatically or not) the forces exchanged between the soil and the individual wheels in order to compensate the effect of external perturbations and preserve the vehicle performance*. Within such a reference frame, the goal of the paper is to study some aspects of the traction control problem by applying the dynamic simulation techniques to a hydrostatic transmission coupled with the simplified model of a 4WD vehicle.

II. System Description

The description of the system under study follows its conceptual development as a combination of two subsystems, i.e. the hydrostatic transmission and the vehicle with the relevant locomotion devices.

A. Hydrostatic transmission

The schematic overview of the hydrostatic transmission used in the application is found in Fig. 1. The main units which work in the closed circuit loop are a variable displacement pump (1) and two variable displacement motors connected in parallel (2 and 3); in fact, this is the minimum number of motors useful to produce the traction control. As well known, the effective operation of the transmission is made possible by the presence of a few additional circuits which perform the following functions: the boost circuit 4 (to maintain one of the two main lines as close as possible to a constant low pressure level), the relief circuit 5 (to bound the pressure in the main lines), and the flushing circuit 6 (to increase the exchange of fluid with the external tank for cooling and filtering).

The functional properties of the transmission depend on the size of the main units, and they should be selected (as a general rule) on the basis of a relatively complex procedure which takes into account the operating envelope of the vehicle and the performance envelope of the units themselves. In this case, however, the type of investigation makes it possible a simpler approach based on a reasonable selection of the relevant parameters. Consequently, a 100 cm^3 (maximum displacement) pump is chosen, running at the constant speed of 2000 rpm, coupled with two 100 cm^3 motors. The displacement setting α_1 of the pump is fully reversible (variable between -1 and +1), while the displacement setting α_2 and α_3 of the motors are variable between 1 (full displacement) and a lower limit of 0.25 according to the standard design of the axial piston units. For convenience, the internal mechanisms which drive the displacement are not detailed but are assumed to be equivalent to first order systems with a time constant of 0.1 second - this choice is due to the relatively slow transients implied by the vehicle motion - and a boundary of 1.0 applied to the absolute value of the time derivative $d\alpha/dt$ to reduce the fluid flow consumption.

The flow and torque losses of the main units are de-

Massimo Martelli works for HP Hydraulic (a manufacturer of hydrostatic transmissions) as supervisor of the electronic control projects. His activity is based at the Institute for Agricultural and Earthmoving Machines (IMAMOTER) of Ferrara, a branch of the National Research Council (CNR). Corresponding author: m.martelli@imamoter.cnr.it

Luca G. Zarotti is Director of the Institute for Agricultural and Earthmoving Machines (IMAMOTER) of the Nation Research Council (CNR) of Italy and Professor of Fluid Power Modelling at the University of Ferrara (Faculty of Engineering).

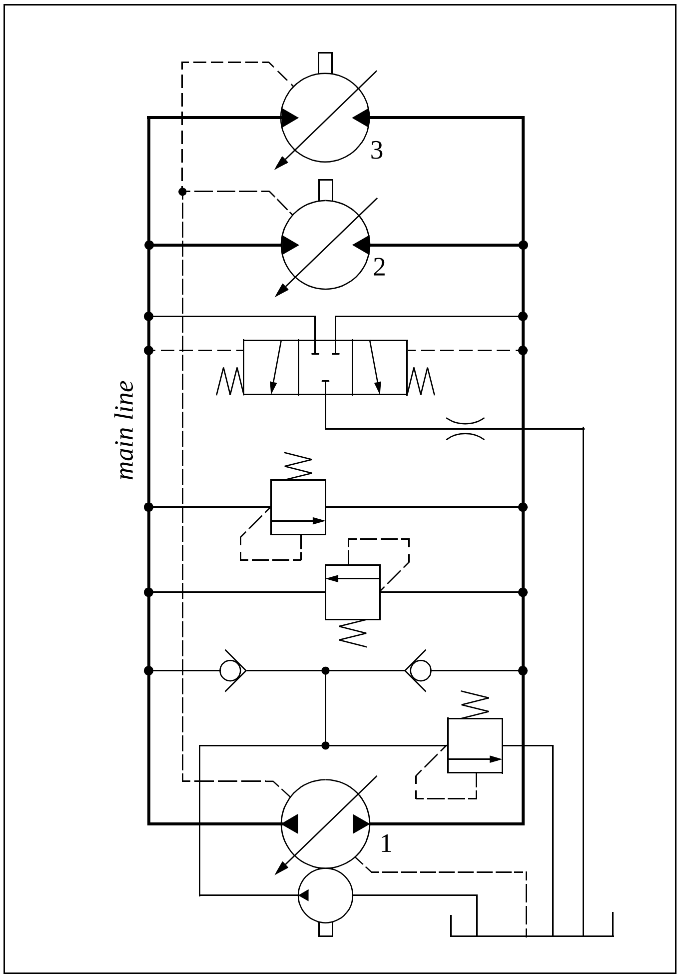

Fig. 1. Schematic of a closed circuit hydrostatic transmission with a variable displacement pump two variable displacement motors in parallel, complemented by the service circuits and valves (boosting and so on).

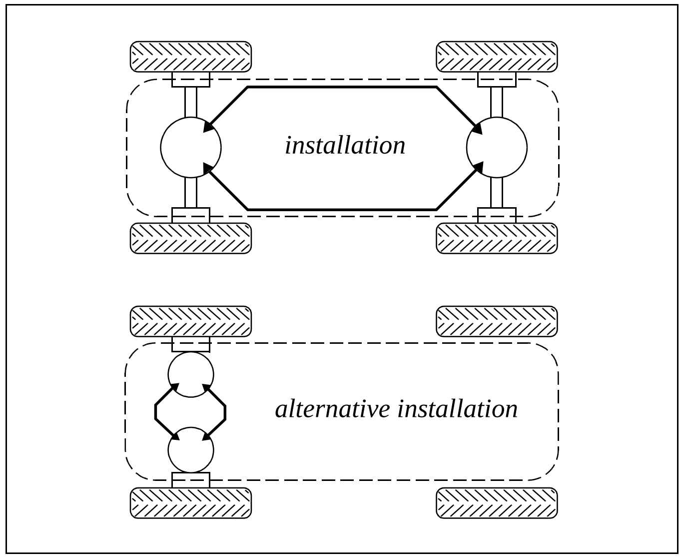

Fig. 2. Possible installation layouts of two hydraulic motors on a vehicle: connected to each axle (top) and connected to the same axle (bottom).

scribed by the generic models presented in [1], which require a limited set of numerical parameters (a total of six) for each unit. The auxiliary components of the transmission, mostly valves of various types, are modelled according to the conventional methods.

B. *Working vehicle*

The vehicle model considered here does not come from the attempt of describing the complete dynamics of the vehicle body and the detailed interface between the terrain and the locomotion devices (i.e. wheels), but its simpler aim is to implement some basic physical concepts and use them as some kind of application oriented environment coupled with the hydrostatic transmission.

The general architecture of the vehicle depends on the number and location of the driving motors. In principle, if two motors are available (see Fig. 1) the options shown in Fig. 2 are possible: (a) one motor drives the front axle through a reduction gear and the second motor drives the rear axle through a second reduction gear; (b) the motors drive the wheels on the same (imaginary) axle through individual reduction gears. In the present investigation the first option is considered - with a reduction ratio of 20:1 - but some aspects of the traction control problem are shared with the second option. The only restrictive assumption to be made - at least at this stage of development - is that the rotational speed of the wheels on each axle are both proportional to the speed of the hydraulic motor.

The layout of the installation of the hydraulic motors is fully compatible with a 2-D model of the vehicle body, i.e. a model where the state variables are the vertical position of the centre of gravity and the pitch angle of the body itself. The latter degree of freedom is due to the deformation of the wheels (or tires) which play a key role in the whole model because they also generate the traction forces. A sketch of the vehicle is shown in Fig. 3 where a few numerical parameters are reported (all lengths are given in mm). Since no special vehicle is reproduced, a symmetrical layout is chosen for reference and the height of the drawbar pull F is taken equal to the height of the CG (center of gravity).In the same Fig. 3 the traction coefficient f_t of the individual wheels is plotted against the wheel slip s in the positive range according to the standard definition of splip as

$$s = \frac{\frac{\omega \cdot R}{\tau} - v}{v} \qquad (1)$$

where ω is the rotational speed of the hydraulic motor, R the effective wheel radius in operation (lower than the nominal radius of Fig. 3), and τ the final reduction ratio between motor and wheel. Though more complex formulas are available, the essentially linear shape of the plot (with a maximum of 0,6 at about 0.15 slip) is chosen to increase the evidence of of the slip effect. The interaction between wheels and terrain is dealt with according to the dynamic model described in [2] where both vertical deformation and horizontal traction are solved by first order differential equations. Finally, the resistance coefficient of the vehicle is 0.03 (constant).

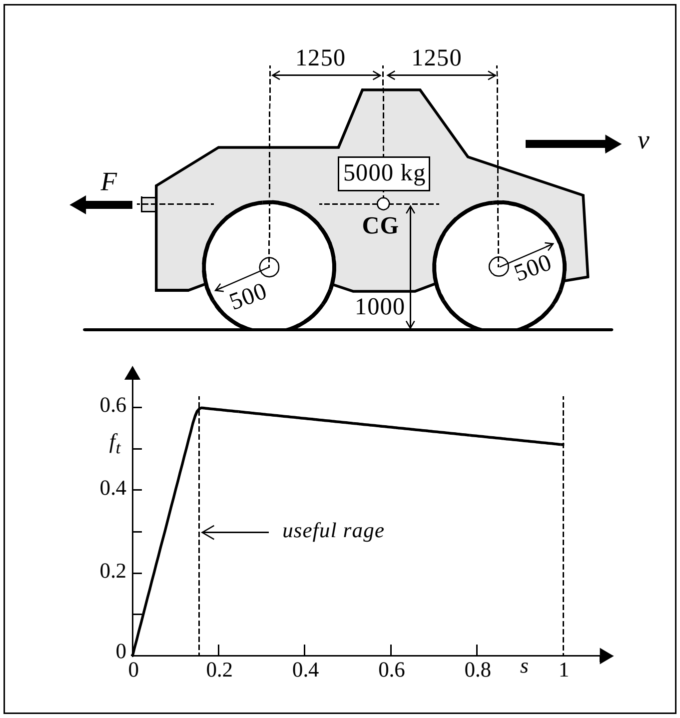

Fig. 3. Sketch of the vehicle used to investigate the traction control in the hydrostatic transmission (dimensions are in mm) complemented by the plot of the traction coefficient of the wheels as a function of slip.

All simulation results reported in the paper have beeen computed by developing the relevant models and solutions in the environment offered by the Easy5 code[3].

C. Overall performance

The performance of the whole assembly of vehicle and transmission (simply named powered vehicle) can be studied in several ways, e.g the simulation of various acceleration and deceleration (braking) transients, simulation of motion uphill or downhill, and so on. The detailed illustration of these topics is out the scope of the paper - though few of them will be implied by the following sections - but it is worthwhile saying that they confirm the general principle that the performance of a hydrostatic transmission has substantial changes when installed on a vehicle and it is hardly predictable by applying artificial loads or interfaces to the transmission.

At least one example of the above principle can be shown deriving the classical description of any transmission (not only the hydrostatic one) through the so called operating envelope, i.e. the boundary curve in the force (drawbar pull)/velocity reference plane which corresponds to a given power on the input shaft. The operating envelope of the powered vehicle considered here is plotted in Fig. 4 where v is the actual vehicle velocity and F is the external drawbar pull. The boundary curve is complemented by two additional plots: the sum of power measurements at the shafts of the hydraulic motors (transmission power), and the final power $F \cdot v$ developed by the vehicle. Though the input power of 60 kW is to a certain extent arbitrary - in fact, both size and behaviour of the prime

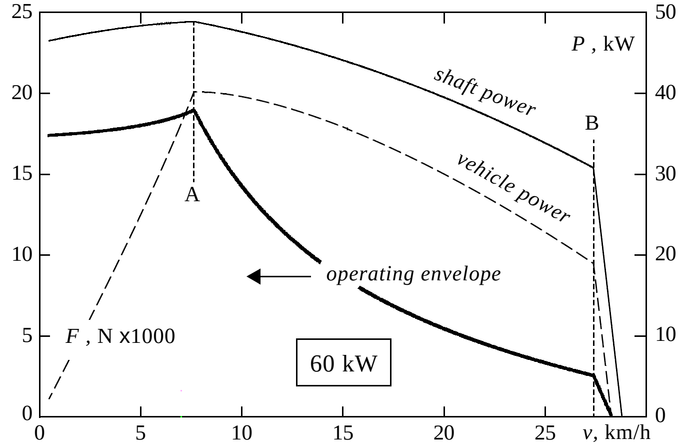

Fig. 4. Operating envelope at 60 kW input of the vehicle plus transmission assembly plotted with the final vehicle power and the intermediate transmission power (computed at the motor shafts).

mover are out of the scope of the investigation - and the actual levels of the plots depend on the numerical models of the system components, the shape of the curves support the following remarks:

1) the traction curve, which is the boundary of the operating envelope, has an intermediate maximum in point A and the same applies to the power plots;
2) the whole traction curve is derived by changing the displacements of the hydraulic motors only, while the pump stays at full displacement;
3) the constant input power is only possible on the left of point B where the hydraulic motors reach their minimum displacement setting;
4) the distance between the vehicle power curve and the transmission power curve increases as the vehicle velocity decreases.

The above effects, which are not visible when a transmission is simulated as a separate system, are all due to the slip of tires and the installation of the transmission on the vehicle. In a real vehicle, a performance as in Fig. 4 would be likely hard to accept but the purpose here is to evidence the extreme impact of the traction interface. For example, a reasonable increase in the traction coefficient (Fig. 3) would improve the performance substantially.

III. Traction Control

The traction control is introduced through a sequence of three steps: the statement of the physical background, the operating principles of two control strategies, and the virtual testing of one of them.

A. Degrees of freedom

The dramatic improvement of the control technology extends, almost every day, the potential applications and the attainable performance of machines (in the wide sense of the term). Though this progress makes it possible to change completely the behavior of a given machine, it is reasonable to think that a control loop would be more simple and reliable if it takes advantage of some native properties of the machine to be controlled.

In the case of the powered vehicle the traction control strategy can take advantage from the native degrees of freedom of the hydrostatic transmission and in particular the displacement settings of the hydraulic motors. In principle this is proved by the expression of the ideal torque T produced by the variable displacement motors, i.e.

$$T_j = \alpha_j \cdot \Delta p \cdot D \qquad j = 2, 3 \tag{2}$$

where Δp is the differential pressure (the same for both motors) and D is their maximum displacement (the same for both motors). If the motor settings α_2 and α_3 are the same the torque is the same, but if the settings are different the front and rear torque are not the same. Consequently, if a final equilibrium of the powered vehicle is reached, the traction forces on the front and rear axle must be different. This theoretical conclusion can be checked against the virtual experiment shown in Fig. 5 where the starting conditions are the following: the pump setting is $\alpha_1 = 1$, the motor settings are $\alpha_2 = \alpha_3 = 0.6$ and the drawbar pull is fixed at 10000 N. The transient plotted refers to a change of the front motor setting from 0.6 to 0.4 and back to the initial value; the change can be done by the operator of the

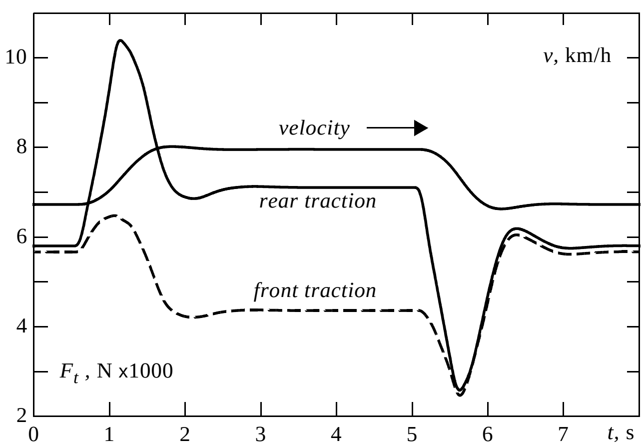

Fig. 5. Virtual experiment of the traction transfer from the front axle to the rear axle by changing the displacement of the front motor from 0.6 to 0.4 and to 0.6 again.

vehicle or by some automatic device. The most important results are the traction curves F_t on the front and rear axle which prove the *traction transfer* between the front and rear axle due to the asymmetrical settings of the motors: this occurs because the slip of the front tires decreases whereas the slip of the rear tires increases (still in the useful range). The steady state pressure in the high pressure line of the transmission increases from a starting value of 180 bar to about 210 bar (an intermediate peak up to 300 bar occurs during the first transient). The change of motor setting can be also positive and, if this occurs, the effects are obviously reversed.

In Fig. 5 the vehicle velocity is also plotted because it gives rise to a potential problem. In fact, while the traction is transferred, the velocity increases - from 13.5 to about 16.0 km/h - as it can be argued by the ideal continuity law applied to the high pressure line of the transmission

$$Q = \alpha_2 \cdot \omega_2 \cdot D + \alpha_3 \cdot \omega_3 \cdot D \tag{3}$$

where Q is flow rate from the pump (constant in the experiment) and ω is the rotational speed of the motor shaft. If the front and rear slip change within relatively small ranges, a significant change in the motor setting increases theor rotational speed and finally the velocity of the vehicle.

Irrespective of the transfer source - change of motor setting done by operator or device - it is to be expected that the side effect on the vehicle velocity has two consequences: (a) the increase of the input power because the drawbar pull does not change during the transient; (b) a negative feeling on the vehicle driver. A simple, though approximate, way to overcome the problem is to associate a 50% automatic change of the pump setting. The potential danger due to the power increase is made clear by considering, for example, that the starting point of the transient in Fig. 5 is located on the operating envelope of Fig. 4; if the input power demand is increased, the boundary of the envelope would be violated and the power balance would be no longer assured.

B. *Operating principles*

Starting from the intermediate conclusion that the installation of a hydrostatic transmission as in Fig. 1 the traction control action means a traction transfer between the front and rear wheels, the control problems becomes equivalent to the investigation of how the transfer can be managed automatically starting from proper inputs received from the vehicle. The most useful way of combining these inputs is the computation of the so called *differential* velocity Δv which is defined as

$$\Delta v = \frac{\omega_3 \cdot R_3}{\tau} - \frac{\omega_2 \cdot R_2}{\tau} \tag{4}$$

where R_j is the actual radius of the wheels in operation and τ is the final reduction ratio (both radius and ratio are not necessarily the same for both axles). The differential velocity has a few interesting properties: (a) if both axles are driving, or positive traction, it is easily proved that Δv is proportional to the difference between the relevant slip values (this is not true if one or both axles are braking, or negative traction); (b) being a difference by definition Δv is not able to qualify the absolute traction capability but the relative capability between the two axles; (c) the sign of Δv can be positive or negative and points to the axle affected by the higher tire slip. The differential velocity is measured in km/h, i.e. the same units of the vehicle velocity which makes easier their direct comparison.

Two particular ideas conceived by some authors on how to use the differential velocity information in view of the development of a traction control system to pilot two variable motors are the following:

1) the first (named here control A) is taken and simplified from the qualitative description found in [4]. In essence, it relates the displacement setting of the individual motors to a continuous control surface. Under

the assumption of a positive Δv a graphical illustration of the control surface is shown in Fig. 6 where the 3D reference space has the following coordinates: the differential velocity, the nominal setting α_{set} of the motor displacement as fixed by the operator, and the motor setting α_2 (the front motor in this case because of the positive range of Δv). Stated that the surface exists only within the active range of the displacement setting $\alpha_{min} \le \alpha_2 \le 1$, the basic features of the control are the following: (a) if Δv is lower than a given threshold Δ_0 nothing happens and the relevant surface is ABCD; (b) if Δv is higher than Δ_0 the displacement setting decreases linearly and the relevant surface is

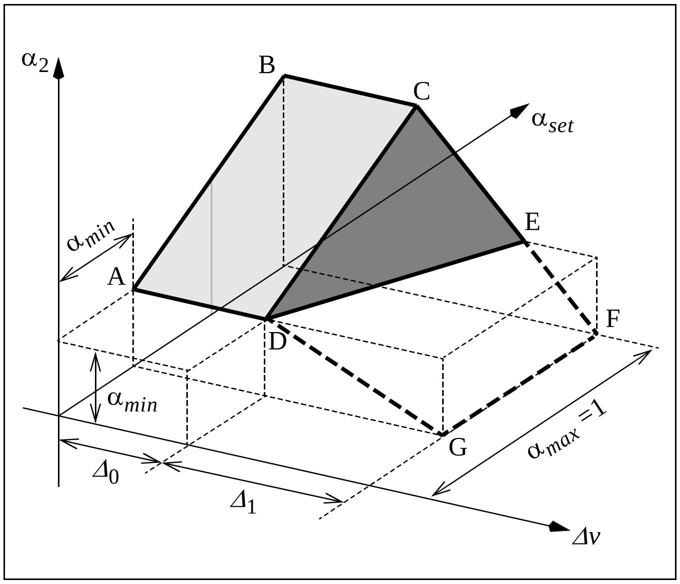

Fig. 6. Three-dimensional plot of the control surface of the front hydraulic motor implemented by control A in the positive range of the differential velocity defined in (4).

CDE which results from the assumption that the motor setting is virtually zero along the FG segment parallel to the α_{set} axis at the total distance $\Delta_0 + \Delta_1$. An alternative control surface could be derived by assuming that the slope of the segment CE is maintained for all points of the segment CD. In the negative range of Δv a similar surface - but not necessarily the same - should be plotted for the displacement setting α_3 of the rear motor;

2) the second idea (named here control B) is taken from the qualitative description given in [5] and shares with control A the presence of a dead-band Δ_0 where the control is not active. Conversely, two differences are found in the control logic: (a) the action on the relevant motor setting is not continuous but discrete or incremental, i.e. $\alpha_{1/2}$ is decreased or increased by a given step $\Delta\alpha$ from the current value; (b) the decision of starting a specific action is taken at the end of a given time cycle Δt which is equal to or multiple of the basic control clock. Clearly, the graphical illustration of Fig. 6 is no longer compatible and should be replaced by a flow chart of logical blocks, which is not reported here because it is still under investigation; in fact the principle seems simple but its implementation is relatively complex specially where it is necessary to base the decision on the records of the past actions.

The fact that both controls drive one motor at a time (instead changing both settings in opposite directions) can be explained by considering that the existence of a margin between the actual setting and the minimum one is more probable than the opposite margin; moreover, a double action would be more critical in view of the overall system stability. Finally, a still open question is the feasibility of similar controls in presence of four parallel motors.

C. *Virtual testing (control A)*

The preliminary step of the virtual testing of any control strategy is the identification of the relevant operating environment. By considering that the tractive effort is the product of the traction coefficient and the vertical force on the wheel, three possible perturbations can be considered to check the control performance:

1) the descrease in the traction coefficient (front or rear) when the powered vehicle is moving on a horizontal surface. This perturbation is perhaps more appropriate to the alternative installation shown at the bottom Fig. 2 but can be possibile on a temporary basis or if the lateral distance of the wheels is not the same;
2) the decrease of the vertical force (front only) when the vehicle is moving on a positive slope. Here the perturbation is the variable slope and is not compatible with alternative installation of motors;
3) the decrease of the vertical force (front only) when the vehicle is moving on a horizonatal surface. This problem, where the perturbation is the drawbar pull, will not be considered in this paper.

First problem - The first problem is studied starting from the steady state conditions which correspond to the traction coefficient of Fig. 3, a drawbar pull of 10000 N, and the following settings of the variable displacement units

$$\alpha_1 = 0.8 \qquad \alpha_2 = \alpha_3 = 0.6 \tag{5}$$

As to the control design, it seems to be fully described (from Fig. 6) by two parameters, i.e. Δ_0 and Δ_1. However, it is reasonable and realistic to think that the control loop is not continuous - due to delays in acquisition, filtering and computation - but it is refreshed at the end of a discrete time cycle Δt (a principle taken here from control B butnot mentioned in [4]). The resulting set of three parameters is then chosen in the following way

$$\Delta_0 = 2 \text{ km/h} \qquad \Delta_1 = 8 \text{ km/h} \qquad \Delta t = 50 \text{ ms} \tag{6}$$

where Δt is the length of control cycle. In Fig. 7 the powered vehicle behaviour is shown as a consequence of the following perturbations: a decrease from 100% to 30% applied in 1 second to the traction curve of the front axle (ON phase), followed by the return in 1 second to the initial or normal curve (OFF phase). The natural plot of the velocity is shown by the “no control” curve which would lead at least to a complete stop of the vehicle. The action of the control, instead, allows a decrease of just 2 km/h

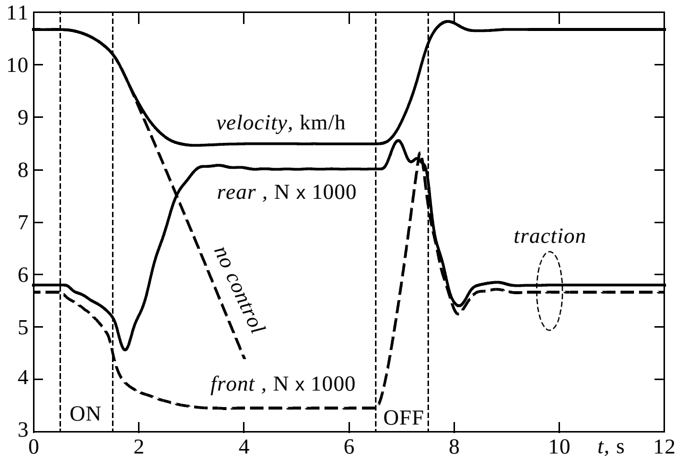

Fig. 7. Virtual experiment of the application of control A to compensate for a reduction from 100% to 30% in the traction coefficient applied to (and subsequently removed from) the front axle of the powered vehicle.

(and this includes the combined reduction of the pump displacement). The associated transfer of the traction forces F_t is significant: in fact, from an almost common value of 6000 N on both axles, the rear axle increases up to about 8000 N and the front axle drops down to about 3500 N. The differential speed Δv is about 0.25 km/h at the beginnig and increases up to about 5 km/h when the control works.

Though the parameters listed in (6) work relatively well in the virtual experiment of Fig. 7, they would require additional sensitivity studies; e.g. to link the Δ_0 threshold to actual velocity of the vehicle. To give just an example, the same experiment of Fig. 7 has been carried out by changing the time cycle Δt from 50 ms to 200 ms. In Fig. 8 the relevant results are compared with those of Fig. 7 by superimposing two couples of plots: the vehicle velocity (top) and the output from the control block to the front motor (bottom). The effect of the longer time cycle is the clear instability of the velocity which is confirmed by the amplitude of the displacement setting (finally saturated by the extreme values of 0,6 and 0,25). The bottom plot also show the discrete operation of the control.

Second problem - The second problem is studied from the steady state conditions which correspond to the traction coefficient of Fig. 3, no drawbar pull, and the increase of the slope from 0 to 22 degrees in five seconds. The results shown in Fig. 9 include the vehicle velocity, the front and rear traction, and the control input to the front motor. The velocity is once again compared with the curve corresponding to the natural behaviour (no control) which would lead to a stop or a reverse drop along the slope. Two remarks are of some interest: (a) the control action starts some time after the final slope is reached, because the differential speed takes some time to develop; (b) though the velocity plot is smooth, the underlying traction force on the rear axle has small oscillations. One of the reasons which explain the latter behaviour is the choice of the control design: in fact the virtual experiment of Fig. 9 has been carried out by changing the Δ_1 parameter from 8 to 12

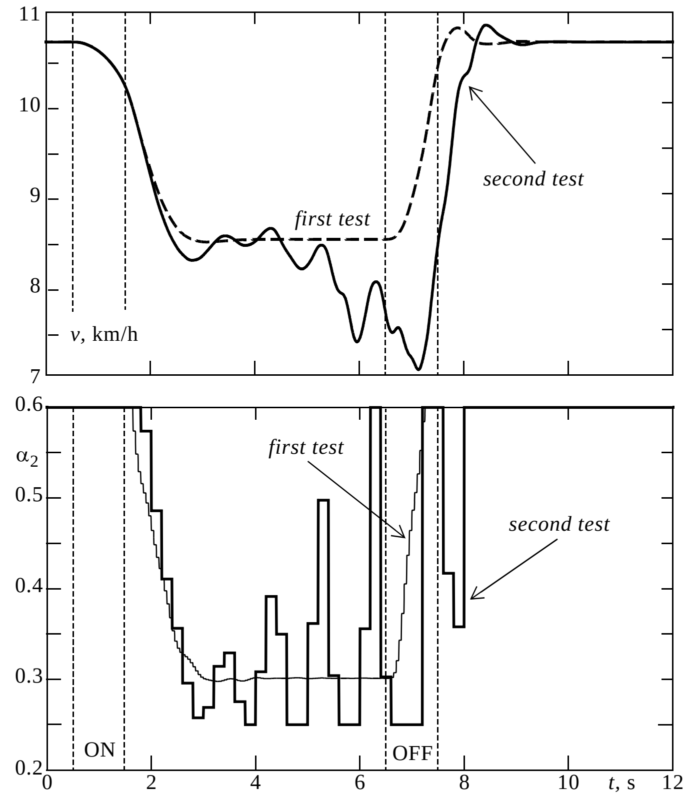

Fig. 8. Virtual experiment (test) of control A carried out with two values of the time cycle (50 and 200 ms) in the same conditions of Fig. 7.

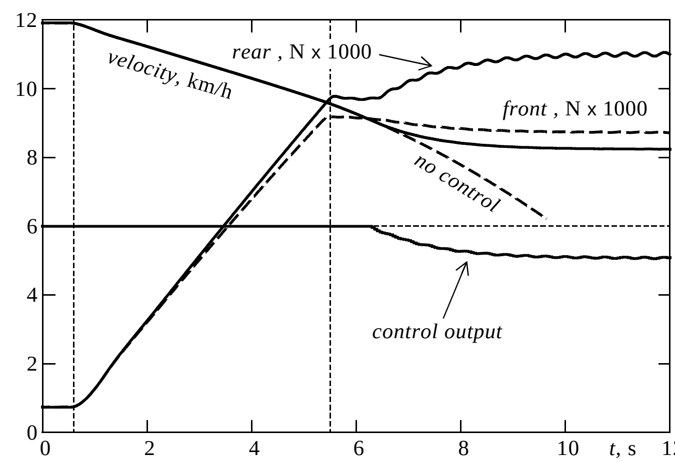

Fig. 9. Virtual experiment of the application of control A during the motion of the powered vehicle along a slope which changes from zero to 22 degrees with no drawbar pull and normal traction coefficient.

km/h because the original value - which worked well when dealing with the first problem - was responsible of a large instability. This suggests that an extended version of the control should take into account the operating conditions and tune the design parameters accordingly.

D. Virtual testing (control B)

As anticipated, the virtual testing of control B is not reported because the relevant strategy is under development. In fact, the critical problem which still lacks a satisfactory solution is the recovery process, i.e. when Δv returns within the range of the acceptable dead-band.

IV. Conclusion

Starting from the numerical model of a powered vehicle equipped with a hydrostatic transmission, the physical principle of the traction transfer between the front and rear axle actuated by means of the displacement setting of the hydraulic motors has been investigated. Based on this principle two proposed traction controls able to operate automatically have been introduced and one of them has been tested in the virtual environment of simulation. The relevant results open the way to additional sensitivity studies helpful to improve the implementation of the control logic and open a larger discussion on the subject.

References

[1] G.L.Zarotti, *Trasmissioni idrostatiche - nozioni e lineamenti introduttivi*, "Quaderni Tematici", No. 5, IMAMOTER-CNR, 2003.

[2] D.A.Crolla, D.N.L.Horton, R.M.Stayner, *Effect of Tyre Modelling on Tractor Ride Vibration Predictions*, Journal of Agricultural Engineering Research, Nr. 47 (1990), pp 55-77.

[3] J.Tollefson, *EASY5 Reference Manual, Boeing*, 1997 (first manual of a complete series). The EASY5 code has been recently transferred to MSC Software.

[4] K.R.Williams, L.T.Jansen, L.A.Jennings, *Traction control system and method for hydraulically propelled vehicles*, Patent 5,775,453.

[5] A.L.Ferguson, C.G.Grembowicz, D.M.Olson, *Traction control apparatus and method for a hydrostatically driven work machine*, Patent 5,924,509.